Supplemental Figures

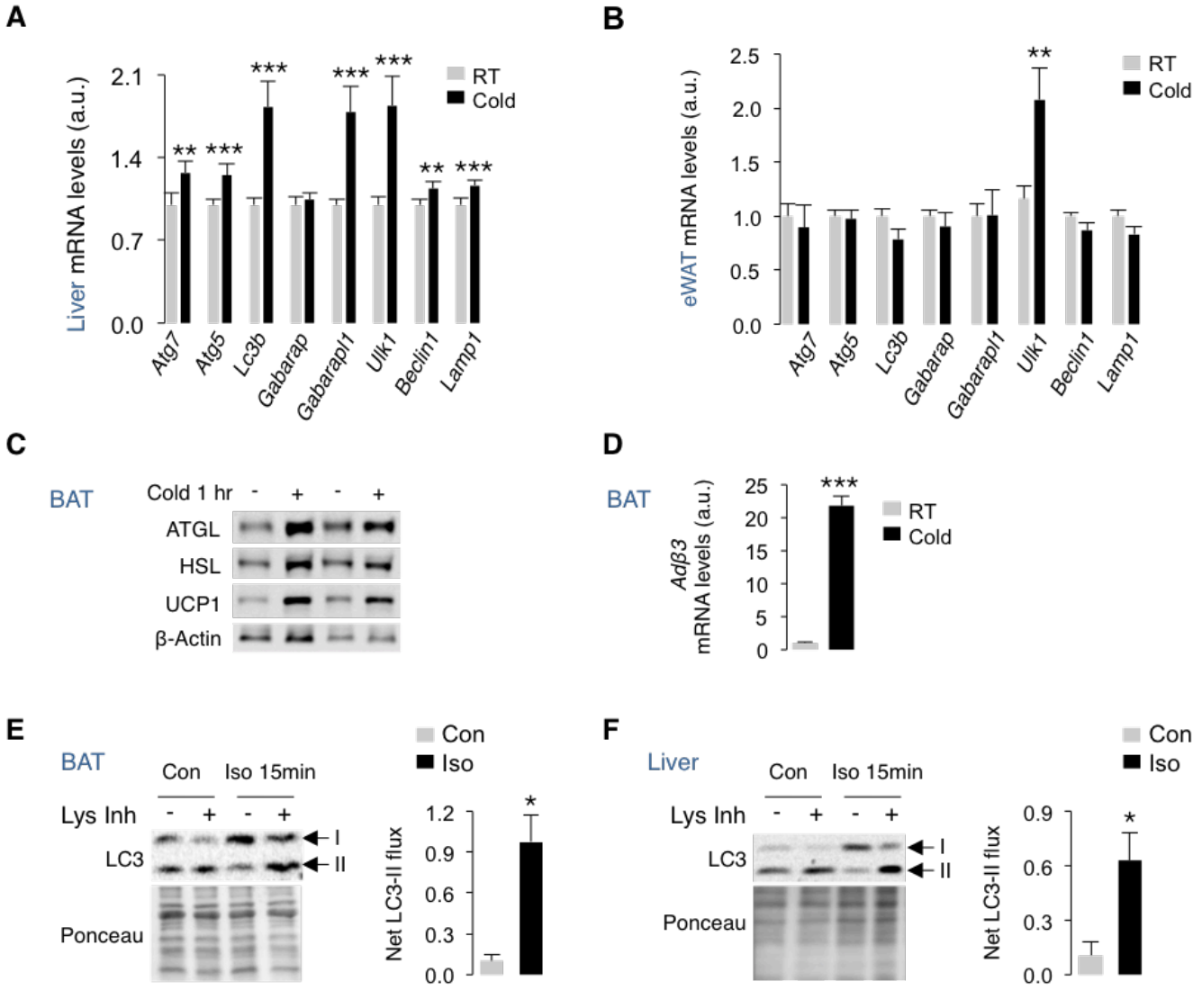

Figure S1, Related to Figure 1. Cold activates autophagy in liver and BAT. (A-B) qPCR for autophagy (*Atg*) genes in liver and epididymal white adipose tissue (eWAT) from room temperature (RT)-housed and 1 hr cold-exposed regular chow-fed 5-6 mo male mice, *n*=4. **(C)** IB for indicated proteins and **(D)** qPCR analyses for *Adβ3* expression in BAT from RT and 1 hr cold-exposed 5-6 mo male mice, *n*=4. **(E)** IB for LC3 in BAT and **(F)** liver from RT-housed mice pre-treated with intraperitoneal (i.p.) Lys Inh for 2 hr and injected i.p. isoproterenol (Iso, 10 mg/kg body weight) for 15 min, *n*=3. Values are mean±s.e.m. **P*<0.05, ***P*<0.01, *** *P*<0.001; Student's *t*-test.

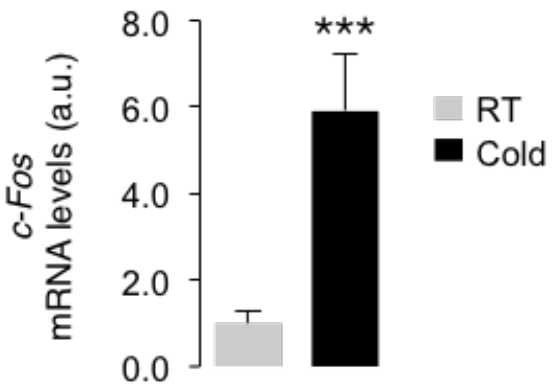

Figure S2, Related to Figure 2. Cold activates hypothalamic autophagy. (A) QPCR analyses for *c-fos* gene expression in the mediobasal hypothalamus from RT-housed and 1 hr cold-exposed regular chow-fed 5-6 mo-old male mice, *n*=4. Values are Mean±s.e.m. *** *P*<0.001; Student's *t*-test.

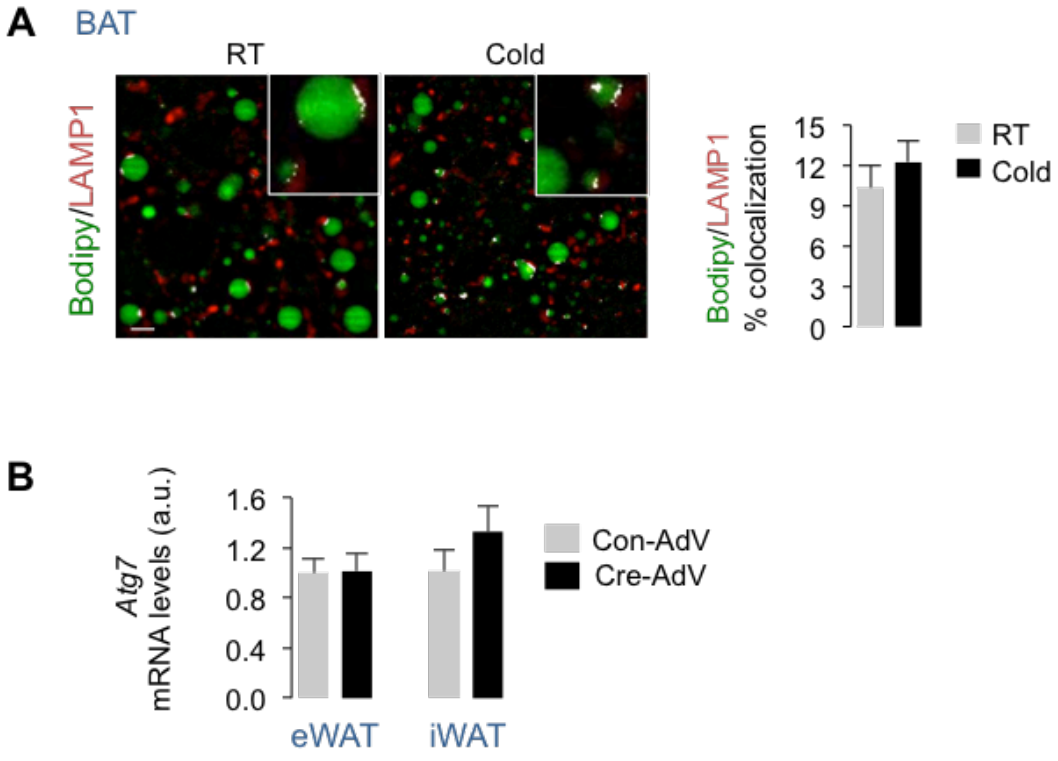

Figure S3, Related to Figure 3. Autophagy degrades LD in BAT. (A) Immunofluorescence for BODIPY and LAMP1 in BAT sections from RT-housed and 1 hr cold-exposed 6 mo old male mice, *n*=3. Scale: 10 μm. **(B)** *Atg7* expression in eWAT and iWAT from $Atg7^{F/F}$ mice injected in BAT with control adenoviruses (Con-AdV) or Cre-expressing AdV (Cre-AdV), *n*=3. Values are mean ± s.e.m., Student's *t*-test.

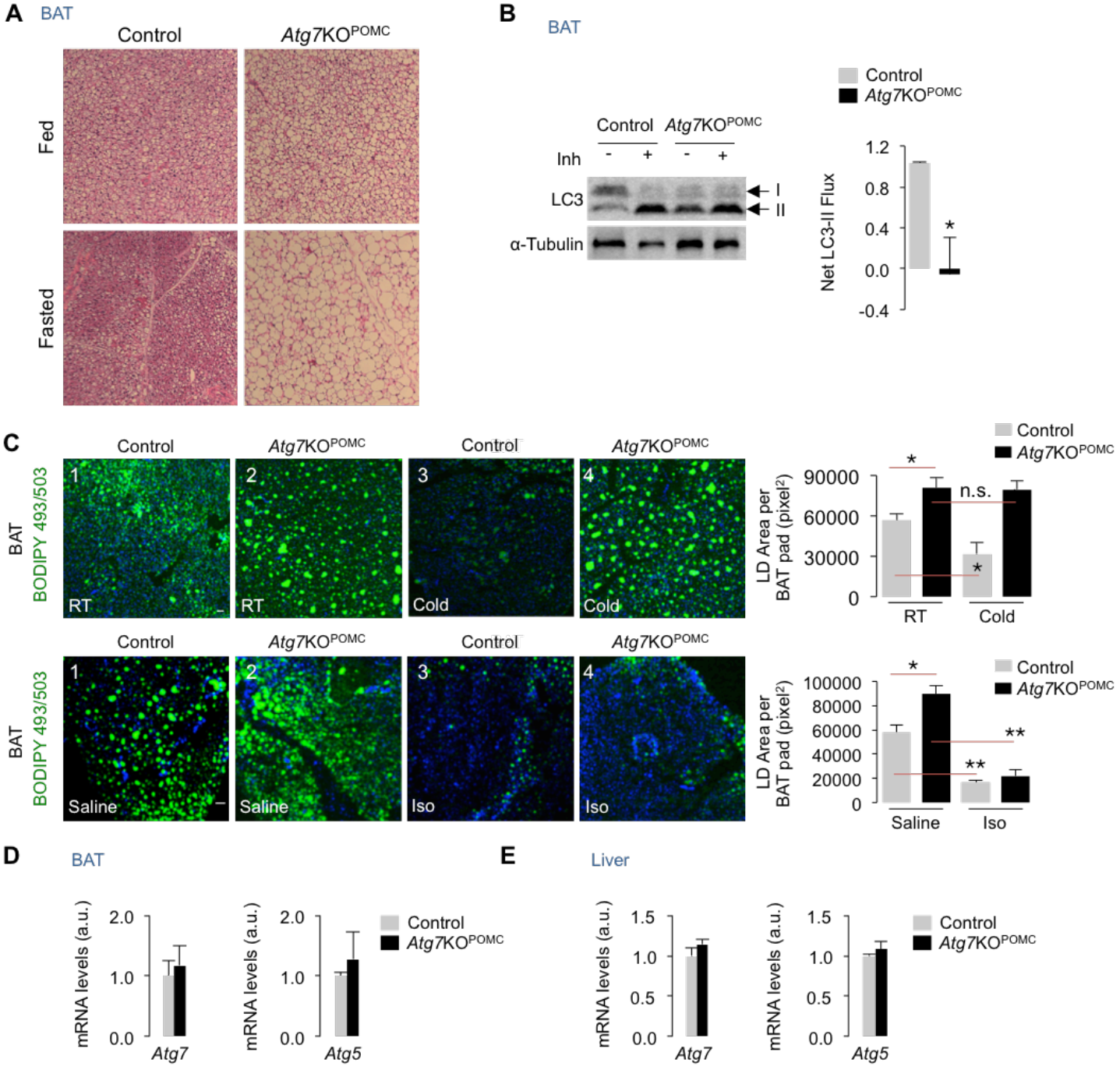

Figure S4. Related to Figure 4. POMCergic autophagy controls lipophagy in BAT. (A) Hematoxylin/Eosin (H&E) stains in BAT from fed and 24 hr fasted 5-6 mo-old male control and *Atg7*KO^{POMC} mice. **(B)** LC3-II flux in BAT treated or not with lysosomal inhibitors (Lys Inh) for 2 hr from 1 hr cold-exposed control and *Atg7*KO^{POMC} 6 mo-old male mice, *n*=3. **(C)** Immunofluorescence (IF) for BODIPY in BAT from room temperature-housed (RT) and 1 hr cold-exposed 6 mo-old male control and *Atg7*KO^{POMC} mice, n=3, and intraperitoneal saline or isoproterenol (Iso, 10 mg/kg body weight for 15 min) injected 4-6 mo-old male control and *Atg7*KO^{POMC} mice, n=3. Scale: 10 μm. **(D-E)** *Atg7* and *Atg5* expression in BAT and liver from 5-6 mo old male control and *Atg7*KO^{POMC} mice, *n*=3. Values are mean ± s.e.m. *P<0.05; Student's t-test.

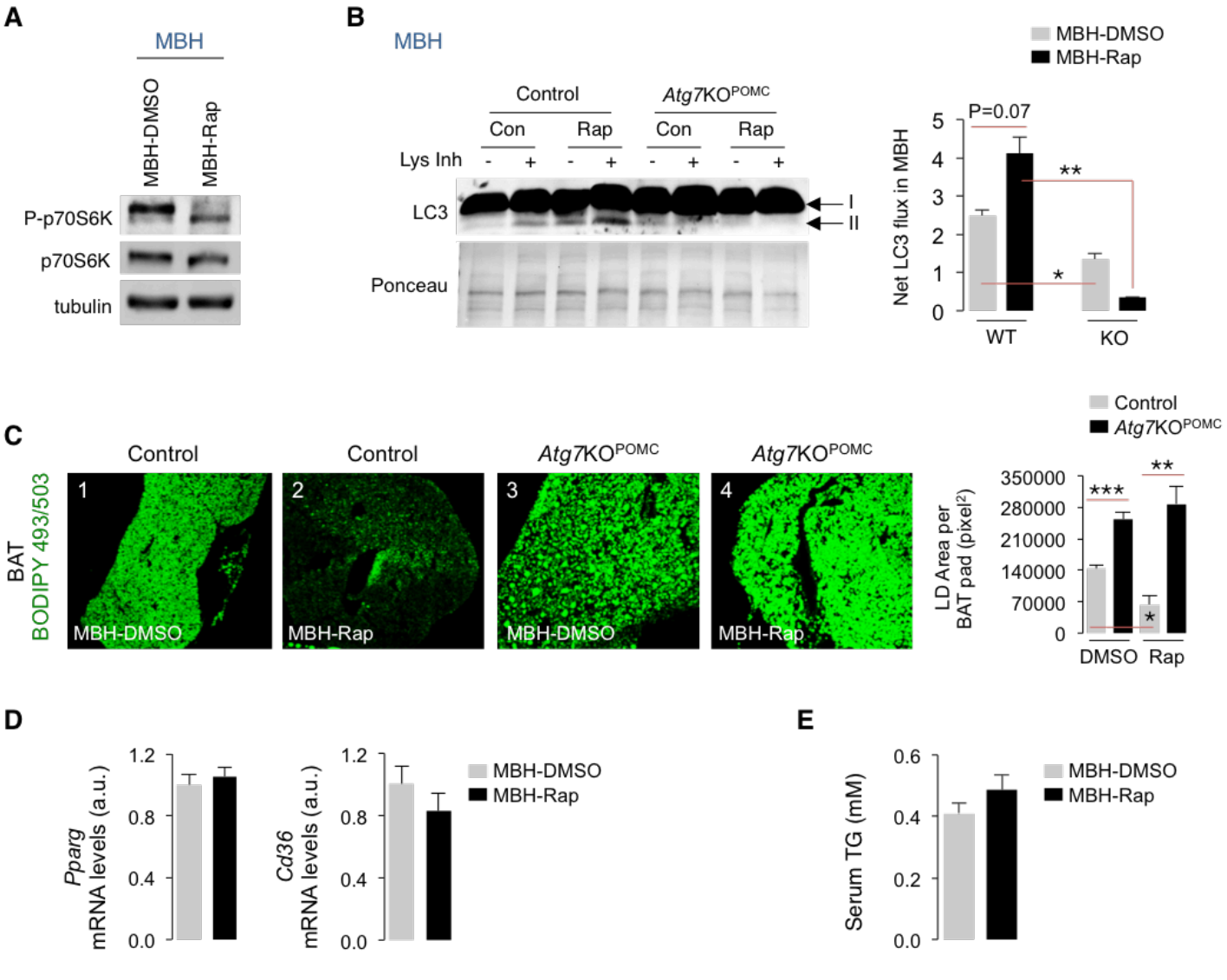

Figure S5. Related to Figure 5. Activation of mediobasal hypothalamic autophagy and depletion of BAT LD by rapamycin. (A) Phospho (P)/total p70SK6 levels in MBH from 6 mo male intra-mediobasal hypothalamus (MBH) DMSO and rapamycin (Rap)-injected mice. **(B)** LC3-II flux in MBH explants from intra-MBH DMSO and Rap injected 5 mo female control and *Atg7*KO^{POMC} mice. Each sample contains MBH from 3 mice, *n*=3. **(C)** BODIPY 493/503 stains in BAT from intra-MBH DMSO or Rap-injected 6 mo male control and *Atg7*KO^{POMC} mice, *n*=5. **(D)** qPCR analyses in liver, and **(E)** serum triglycerides (TG) from intra-MBH DMSO and Rap-injected 6 mo male mice, *n*=5. Bars are mean±s.e.m. **P*<0.05, ***P*<0.01, ****P*<0.001; Student's *t*-test. Values are mean ± s.e.m.

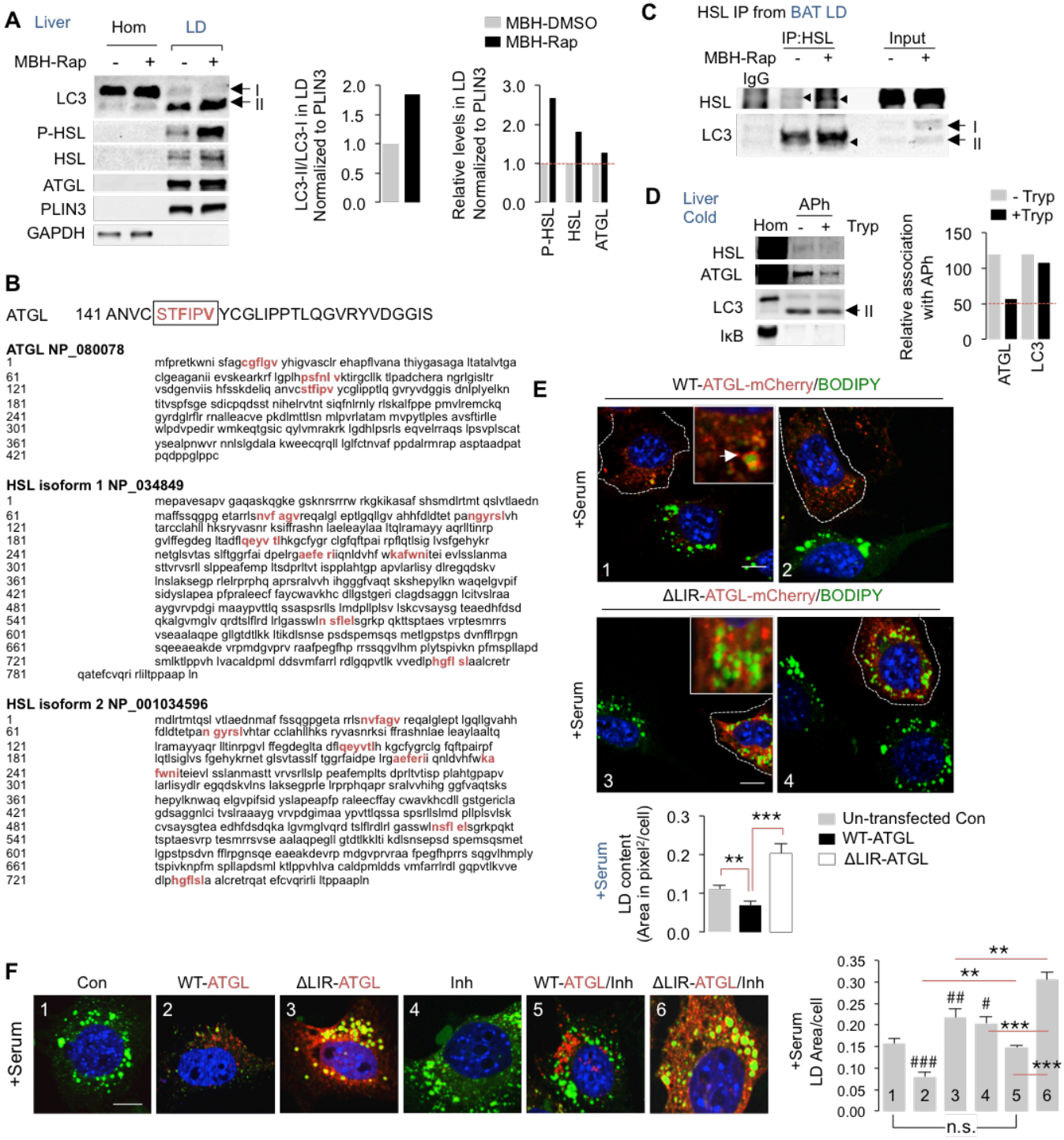

Figure S6. Related to Figure 7. Lipases require LIR motifs for lipolysis. (A) Immunoblots for indicated proteins in liver homogenates (Hom) and LD from intra-MBH DMSO or Rap injected mice. Quantifications for LC3-II/LC3-I and indicated proteins in LD normalized to PLIN3 (5 BAT pads pooled per sample, *n*=2). **(B)** ATGL and HSL contain LC3-interacting region (LIR) motifs (shown in red). **(C)** HSL-LC3 co-IP in BAT LD from intra-MBH DMSO or Rap-injected mice. **(D)** Autophagosomes **(**APh) from livers from cold-exposed mice subjected to LC3 trypsin protection assay (5 livers pooled per sample, *n*=2), and IB for indicated proteins, *n*=2. **(E** and **F)** Direct fluorescence for mCherry/BODIPY in serum-fed NIH3T3 cells expressing mCherry-positive WT-ATGL or ΔLIR-ATGL treated with (0.25 mM) OA -/+ lysosomal inhibitors (Inh) for 6 hr. Dotted lines outline transfected cells. LD content depicted as area (pixel^2) per cell. At least 40 cells were analyzed from *n*=3. Scale: 10 μm. Bars are mean±s.e.m. **P*<0.05, ***P*<0.01, ****P*<0.001, ($^{\#}$*P*<0.05, $^{\#\#}$*P*<0.01, $^{\#\#\#}$*P*<0.001 compared to panel 1 in F), Student's *t*-test.

Supplemental Experimental Procedures

Fluorescence microscopy

Cells were fixed on coverslips with a 4% paraformaldehyde (PFA) solution, and blocked and incubated with primary and secondary antibodies (Alexa Fluor 488 and/or Alexa Fluor 647 conjugated) (Invitrogen). For lipid droplet (LD) detection, cells were incubated with BODIPY 493/503 for 20min at RT. Frozen MBH sections from 4% PFA-perfused mice or BAT sections (5μm thick) were fixed in 3% PFA in 1x PBS for 10 minutes and blocked with 3% horse serum, 1% BSA in 1x PBS containing 0.4% triton X-100 for 1 hour at room temperature. Mounting medium contained DAPI (4', 6-diamidino-2-phenylindole) to visualize the nucleus (Invitrogen). Images were acquired on a Leica DMI6000B microscope/DFC360FX 1.4-megapixel monochrome digital camera (Leica Microsystems, Germany) using X63 or X100 objective/1.4 numerical aperture. Images were acquired at similar exposure times in the same imaging session. Image slices of 0.2μm thickness were acquired and deconvolved using the Leica MetaMorph acquisition/analysis software. All images were subjected to identical post-acquisition processing. Quantification was performed in deconvolved images after appropriate thresholding using the ImageJ software (NIH) (Schneider et al., 2012) in a minimum of 30 cells or as otherwise indicated for specific experiments from at least 2 experiments. Cellular fluorescence intensity was expressed as mean integrated density as a function of individual cell size. Percentage colocalization was calculated using the JACoP plugin in single Z-stack sections of deconvolved images. Colocalization is shown in native images and/or as white pixels using the "colocalization finder" plugin in ImageJ (Schneider et al., 2012). LD area is represented as pixel^2.

RNA isolation and qPCR analyses

Total RNA was isolated as previously described (Martinez-Lopez et al., 2013).

The following primers were used:

Adβ3	forward (f) 5'-ggcaacctgctggtaatcat-3'	reverse (r) 5'- tccactgacgtccacagttc-3'
Atg3	(f) 5'-gcagacatggaagaatatgaag-3'	(r) 5'-ggtgtctggtaatatttgtcg-3'
Atg4b	(f) 5'-tgggtgttattggagggaag-3'	(r) 5'-cagaaaaaccccacagcaat-3'
Atg5	(f) 5'-tagaatatatcagaccacgacg-3'	(r) 5'-ctcctcttctctccatcttc-3'
Atg7	(f) 5'-tccgttgaagtcctctgctt-3'	(r) 5'-ccactgaggttcaccatcct-3'
Beclin1	(f) 5'-ggccaataagatgggtctga-3'	(r) 5'-gctgcacacagtccagaaaa-3'
Cd36	(f) 5'-tgctggagctgttattggtg-3'	(r) 5'-tgggttttgcacatcaaaga-3'
c-Fos	(f) 5'-ggggcaaagtagagcagcta-3'	(r) 5'-ggctgccaaaataaactcca-3'
Gabarap	(f) 5'-gtcccggtgatagtggaaaa-3'	(r) 5'-tgggtggaatgacattgttg-3'
Gabarapl1	(f) 5'-tcgtggagaaggctcctaaa-3'	(r) 5'-atacagctggcccatggtag-3'
Gabarapl2	(f) 5'-tctcgggctctcagattgtt-3'	(r) 5'-gtgttctctccgctgtaggc-3'
Lc3b	(f) 5'-acaaagagtggaagatgtccggct-3'	(r) 5'-tgcaagcgccgtctgattatcttg-3'
Lamp1	(f) 5'-tagtgcccacattcagcatctcca-3'	(r) 5'-ttccacagacccaaacctgtcact-3'
Pnpla2 (ATGL)	(f) 5'-atttatcccggtgtactgtggcct-3'	(r) 5'-agtggcaagttgtctgaaatgccg-3'
Pparg	(f) 5'-aatccttggccctctgagat-3'	(r) 5'-ttttcaagggtgccagtttc-3'
Tbp	(f) 5'-gaagctgcggtacaattccag-3'	(r) 5'-ccccttgtaccttcaccaat-3'
Tfeb	(f) 5'-gcggcagaagaaagacaatc-3'	(r) 5'-ctgcatcctccggatgtaat-3'
Ucp1	(f) 5'-actgccacacctccagtcatt-3'	(r) 5'-ctttgcctcactcaggattgg-3'
Ulk1	(f) 5'-agattgctgactttggattc-3'	(r) 5'-agccatgtacataggagaac-3'

Plasmids

Transient transfections were performed with Lipofectamine 2000 (Invitrogen) as per the manufacturer's instructions. ATGL plasmid was a kind gift from Dr. Carole Sztalryd Woodle (University of Maryland School of Medicine), and site-directed mutagenesis was used to introduce F147A and V150A mutations using a commercial kit (Life Technologies).

Histological analyses

The Histology and Comparative Pathology core at the Albert Einstein College of Medicine performed histological analyses. Paraffin-embedded sections (5μm thick) of formalin-fixed tissues were subjected to Hematoxylin and Eosin (H&E). Sections were analyzed under a Nikon light microscope at the indicated magnification and quantified with ImageJ software (NIH, USA).

Bioenergetics
Tissue bioenergetics was determined using a Seahorse respirometer (Cypess et al., 2013). Briefly, BAT and liver were collected rapidly after sacrifice, and rinsed with Krebs-Henseleit buffer (KHB) (111mM NaCl, 4.7mM KCl, 2mM $MgSO_4$, 1.2mM Na_2HPO_4, 0.5mM carnitine, 2.5mM glucose and 10mM sodium pyruvate). Tissues were cut into small pieces (6-10mg) and quickly transferred to individual wells of a XF24 plate. Individual pieces were stabilized from excessive movement by islet-capture screens (Seahorse Bioscience), and 450μL KHB was added to each well. Digitonin was added to enhance plasma membrane permeability. Basal oxygen consumption rates (OCR) were determined according to the following plan: Basal readings recorded every 2min for 10 readings, followed by exposure to digitonin. Subsequent readings were recorded after 2min mixing and 2min rest. Basal OCR values were normalized to individual tissue weights.

Autophagosome isolation and LC3-II protease protection assay
Autophagic vacuoles (APh) were isolated from mouse livers and BAT by differential centrifugation using discontinuous density gradients of metrizamide (Marzella et al., 1982). Tissue homogenates were centrifuged at 2,000 g, 5 min followed by centrifugation of supernatant at 43,000 rpm for 12 min. Pellets were suspended in 1.9 mL 0.25 M sucrose, and then 2.8 mL metrizamide (85.6%) was added. Samples were centrifuged on a 26 % - 24 % - 20 % - 15 % metrizamide gradient at 24,700 rpm for 3 hr. APh fraction was collected from the 15-20% interface. APh fraction was centrifuged at 24,000 g and pellets were suspended in 0.25 M sucrose and used for assays. For the LC3-II protease protection assay (Nair et al., 2011), freshly isolated APh was incubated in presence or absence of 0.5 μg of trypsin (Sigma-Aldrich, MO, USA) at room temperature for 15 minutes. Samples were quickly boiled in 2X SDS-PAGE sample buffer at 95 ºC for 5 min and resolved by SDS-PAGE. APh samples were analyzed for levels of ATGL, HSL, LC3 and IκB. ATGL and HSL levels were normalized to LC3-II and compared to total levels in corresponding trypsin-untreated control fractions.

Core body temperature measurements
Body temperature (°Celsius) was measured with a rectal thermometer (BIOSEB, Pinellas Park, FL) inserted 1 cm into the rectum and allowed to stabilize for 5 seconds and values were recorded as indicated (Martinez-Lopez et al., 2013). Rodents were sacrificed if core body temperature dropped below 25°C. Briefly, mice were individually housed in cages (without nestlets) and placed in refrigerated rooms at ~4°C temperature for 1 hr. Mice were individually housed in similar cages without nestlets in the absence of food for 1 hr at RT but free access to water. Mice were sacrificed immediately after the cold challenge.

General methods
MBH, BAT and liver proteins were generated using a lysis buffer containing protease and phosphatase inhibitors and subjected to Western blot analysis, as described (Singh et al., 2009b).

Supplemental References

Martinez-Lopez, N., Athonvarangkul, D., Sahu, S., Coletto, L., Zong, H., Bastie, C.C., Pessin, J.E., Schwartz, G.J., and Singh, R. (2013). Autophagy in Myf5+ progenitors regulates energy and glucose homeostasis through control of brown fat and skeletal muscle development. EMBO reports *14*, 795-803.

Marzella, L., Ahlberg, J., Glaumann, H. (1982). Isolation of autophagic vacuoles from rat liver: morphological and biochemical characterization. *Journal of Cell Biology* **93**, 144-154.

Nair, U., Thumm, M., Klionsky, D.J., and Krick, R. (2011). GFP-Atg8 protease protection as a tool to monitor autophagosome biogenesis. Autophagy *7*, 1546-1550.

Schneider, C.A., Rasband, W.S., and Eliceiri, K.W. (2012). NIH Image to ImageJ: 25 years of image analysis. Nature methods *9*, 671-675.

Singh, R., Kaushik, S., Wang, Y., Xiang, Y., Novak, I., Komatsu, M., Tanaka, K., Cuervo, A.M., and Czaja, M.J. (2009a). Autophagy regulates lipid metabolism. Nature *458*, 1131-1135.

Singh, R., Xiang, Y., Wang, Y., Baikati, K., Cuervo, A.M., Luu, Y.K., Tang, Y., Pessin, J.E., Schwartz, G.J., and Czaja, M.J. (2009b). Autophagy regulates adipose mass and differentiation in mice. The Journal of clinical investigation *119*, 3329-3339.